Series Transformer-Based Solid State Fault Current Limiter

Hamid Radmanesh, *Associate Member, IEEE,* Hamid Fathi, *Member, IEEE,*
Gevork B. Gharehpetian, *Senior Member, IEEE*

***Abstract*—This paper studies a novel transformer-based solid state fault current limiter (TBSSFCL) for radial distribution network applications. The proposed TBSSFCL is capable of controlling the magnitude of fault current. In order to control the fault current, primary winding of an isolating transformer is connected in series with the line and the secondary side is connected to a reactor, paralleled with a bypass switch which is made of anti-parallel insulated gate bipolar transistors. By controlling the magnitude of ac reactor current, the fault current is reduced and voltage of the point of common coupling is kept at an acceptable level. Also, by this TBSSFCL, switching overvoltage is reduced significantly. The proposed TBSSFCL can improve the power quality factors and also, due to its simple structure, the cost is relatively low. Laboratory results are also presented to verify the simulation and theoretical studies. It is shown that this TBSSFCL can limit the fault current with negligible delay, smooth the fault current waveform, and improve the power quality.**

***Index Terms*—Fault current limiter (FCL), isolating transformer, point of common coupling (PCC), power quality, short circuit current, voltage sag.**

I. Introduction

DEVELOPING power system networks and their interconnections may increase the short-circuit levels beyond the capacity of circuit breakers (CBs). Short-circuit fault can cause overvoltage transients, loss of synchronization, and isolation failure and may cause explosion of equipments containing insulating oil. There are solutions such as upgrading or replacing switchgears [1], which are expensive. Distribution network protection mainly relies on proven protection devices such as fuse. This equipment is a self-triggering, cheap, small size, and reliable protective device which can interrupt fault currents without using sensors and actuators [2]. But, it is a single-use device and needs manual replacement. Employing high impedance transformer to increase the fault circuit impedance is another solution, which causes additional network losses and needs redesign for maintaining the voltage profile [3]. CB is also a protective device, which can be tripped and reset manually or automatically. However, CBs with high-current interrupting capability are expensive electromechanical systems [3]. Replacement of protective CBs is a costly solution to cope with rising fault current levels. In recent years, a novel scheme for limiting the magnitude of fault current, the so called "fault current limiter" (FCL), has been proposed and used as the best solution. This scheme can limit the fault current, dismissing the costly upgrade of switchgears. FCLs application in distribution networks not only suppresses the fault current and limits the inrush current, but also improves the transient stability, power quality, and reliability [4]–[8]. Development of various types of FCLs has been conducted for many years by many research institutions around the world. Solid-state FCL (SSFCL) is a power electronic-based device with fast response in fault current limiting. SSFCLs have been classified into three major groups: 1) the series switch (mechanical or semiconductor) [9]; 2) the bridge [10]–[12]; and 3) resonant structure types [13]. A single-phase FCL employing insulated gate bipolar transistor (IGBT)-based bidirectional switch can be realized by using a stack of IGBTs, an anti-parallel diode, and varistors connected in parallel with the switches for voltage clamping [14]. Bridge-type FCLs with reduced number of controlled devices have been presented in [15], in which single-phase and three-phase four-wire configurations have been proposed. Its fast response allows the cost, weight and volume of the reactor to be reduced. The effect of controllable resistor type FCL on voltage sag and fault current has been studied in [16], where a damping resistor is inserted into the transmission line, via IGBT switch and isolation transformer. The suggested structure can improve the voltage profile up to an acceptable level, but overvoltage on the IGBT is considerable. Application of superconducting FCL (SFCL) in loop power distribution systems for voltage sag analysis has been considered in [17]. In order to overcome the problems raised by distributed generation (DG), static FCL (SFCL) has been proposed in [18]. SFCL can decrease fault current level and improve power quality during fault. In addition, FCL effect on the distribution networks protection in the case of installed DG has been studied in [19]–[21]. In [22] a radial distribution network is considered for comparison of the performance of two SSFCLs, regarding the fault current and power quality. The effect of SSFCL on the fault current in a single-source radial system, as well as a multiple source distribution system with a bus-tie has been presented in [23]. Study of electrical system with SFCL connected in series with the feeder has been performed in [24]. This system uses fiber optic communication to coordinate the operation of fault interrupting switches, located along the circuit.

Manuscript received May 16, 2014; revised September 23, 2014 and December 2, 2014; accepted January 20, 2015. Paper no. TSG-00402-2014.

The authors are with the Department of Electrical Engineering, Amirkabir University of Technology (Tehran Polytechnic), Tehran 1995755681, Iran (e-mail: hamid.radmanesh@aut.ac.ir).

Color versions of one or more of the figures in this paper are available online at http://ieeexplore.ieee.org.

Digital Object Identifier 10.1109/TSG.2015.2398365

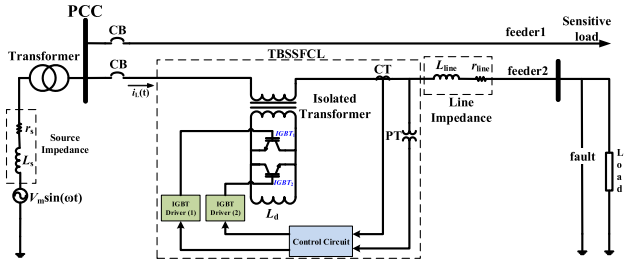

Fig. 1. Single line diagram of a double feeder radial distribution network including the proposed TBSSFCL.

A new hybrid type FCL topology for use in distribution systems has been proposed in [25]. This paper employs pulse-width modulation technique to control the fault current. Quantitative analysis for FCLs, high temperature superconductor cables and transformers, in the world market, has been made in [26].

Regarding their protective reaction, FCLs can be divided into two types. One type limits the fault current to an acceptable level, which can be safely interrupted by CB. The other type acts as a breaker and interrupts the fault current itself.

In this paper, the first type, i.e., noninterrupting FCL, is investigated. The proposed transformer-based solid state FCL (TBSSFCL) has a simple structure, which can limit the magnitude of fault current to some safe value. In addition to restoring the point of common coupling (PCC) voltage, it is capable of reducing harmonic distortion and switching overvoltage, as compared to the five newly proposed FCLs in [4], [6], [12], [16], and [27]. The TBSSFCL operations in normal and faulty conditions are studied. An experimental prototype is also developed and tested, the results of which clearly confirm the simulation results. It is shown that the proposed TBSSFCL has a simple and cheaper structure, while acting better, as compared with the above mentioned FCLs.

This paper is organized as follows.

In Section II, the system topology is discussed. Then, in Section III, the proposed TBSSFCL topology is introduced and its operation in a simplified single line radial distribution network is explained. In this section, analytical study of PCC voltage sag, TBSSFCL power losses and control system are presented. In Section IV, MATLAB software is employed to investigate the operational behavior of TBSSFCL and related simulation results are analyzed. In Section V, experimental results are presented and finally the conclusion is given in Section VI.

II. System Topology

Single line diagram of a double feeder radial distribution network, including the proposed TBSSFCL, is shown in Fig. 1. It is assumed that the feeder F1 supplies a sensitive load and the feeder F2 delivers power to other loads.

The TBSSFCL is composed of three main parts as described below.

An isolating transformer with unity turn ratio, the primary winding of which is connected in series with the line. The secondary winding of this transformer is connected to an anti-parallel IGBTs switch in parallel with a nonsuperconductor (copper) coil which serves as an ac reactor, modeled by L_d in Fig. 1. The parallel connection of IGBTs and ac reactor forms a fault current amplitude controller and, together with the series transformer constitute the TBSSFCL.

III. TBSSFCL Operation Principles

In normal operation mode IGBTs are on, so the secondary winding is short circuited and there is negligible voltage drop on primary side of the transformer. In this case, TBSSFCL shows negligible impedance and has little effect on power quality. At fault inception, monitoring system recognizes the fault and turns off the anti-parallel IGBTs. Therefore, the bypass path is removed and the secondary circuit is closed through the ac reactor. This results in increased impedance of the TBSSFCL, which limits the fault current to some acceptable level.

A. Circuit Analysis

According to the value of the feeder current, TBSSFCL operates in two modes. In normal operation mode, when the system operates at steady state, as well as at the fault inception, that the fault current is less than a prespecified value I_L, IGBTs are on, causing a voltage drop in the order of a few volts (2 V for the IGBTs used in this paper). In addition, the series transformer would not normally have leakage impedance of more than 3–4%. Therefore, the total voltage drop across the TBSSFCL would be negligible and is not taken into account, in this paper. The other mode corresponds to the fault condition, when the feeder current exceeds I_L. In this mode, IGBTs are in off state and the fault current is limited by TBSSFCL. During the normal mode, ac reactor current is zero and the line current is given by

$$V_m \sin(\omega t) = L\frac{di_L(t)}{dt} + Ri_L(t) \tag{1}$$

where R and L include the source, line, and load resistances and inductances and the source voltage of the electrical network is assumed sinusoidal. In this case, the system is in steady state, i.e., the transient component of current has already been damped. Therefore, the solution of (1) is as given in

$$i_L(t) = \frac{V_m}{\sqrt{R^2+\omega^2L^2}} \sin\left(\omega t - \tan^{-1}\frac{\omega L}{R}\right). \tag{2}$$

In fault condition, the line current increases rapidly and exceeds I_L, by which the controller turns-off the anti-parallel IGBTs and connects the ac reactor to the feeder. During fault mode, the ac reactor charges according to (1), but with the values of L and R including TBSSFCL inductance and resistance and excluding the short circuited load parameters. Solving (1) for the fault condition yields

$$i_L(\omega t) = Ae^{-\frac{R}{L\omega}\omega(t-t_1)} + B\sin(\omega t - \varphi) \tag{3}$$

where

$$\left\{A = \frac{-V_m}{\sqrt{R^2+\omega^2L^2}},\ B = \frac{V_m}{\sqrt{R^2+\omega^2L^2}},\ \varphi = arc\tan\left(\frac{\omega L}{R}\right).\right.$$

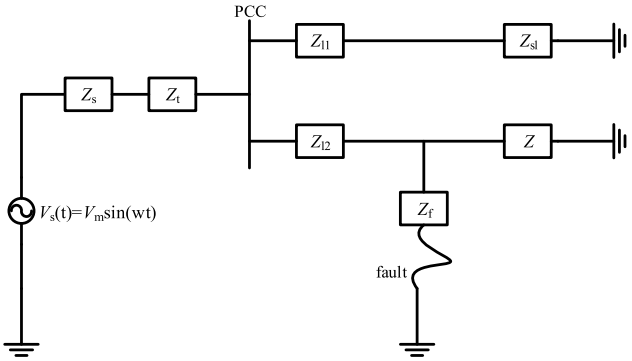

Fig. 2. Positive sequence equivalent circuit of the radial distribution network during fault.

Equation (3) is composed of exponential and sinusoidal terms. The exponential term indicates a transient in the line current, duration of which (from t_1 to t_2 in Fig. 6) depends on the system time constant (L_d/R), where R is the system resistance seen by the ac reactor.

B. Voltage Sag Studies

When fault occurs in feeder2, it causes voltage sag at PCC. For voltage sag analysis, positive sequence equivalent circuit of the faulted system is shown in Fig. 2. To analyze voltage sag, the method introduced in [28] is used. In the normal operation mode, PCC voltage magnitude $V_{\mathrm{PCC}(N)}$ and its phase angle $\varphi_{\mathrm{PCC}(N)}$ can be expressed by

$$V_{\mathrm{PCC}(N)} = \left| \frac{\bar{Z}_{K(N)}}{\left(\bar{Z}_S + \bar{Z}_t\right) + \bar{Z}_{K(N)}} \right| \left|\bar{V}_S\right| \tag{4}$$

$$\varphi_{\mathrm{PCC}(N)} = \arctan\left(\frac{X_{K(N)}}{R_{K(N)}}\right) - \arctan\left(\frac{X_{K(N)} + X_S + X_t}{R_{K(N)} + R_S + R_t}\right). \tag{5}$$

The phase angle of $\bar{V}_S$ is assumed to be zero. $\bar{Z}_t$ is the transformer impedance phasor, $\bar{Z}_S = R_S + jX_S$ is the source impedance phasor and $\bar{V}_S$ is source voltage phasor all in normal operation mode. By considering the parallel feeders' impedance in normal operation mode, (6) can be written

$$\bar{Z}_{K(N)} = R_{K(N)} + jX_{K(N)} \tag{6}$$

where

$$Z_{K(N)} = \left(\bar{Z}_{L1} + \bar{Z}_{SL}\right) \| \left(\bar{Z}_{L2} + \bar{Z}\right) \tag{7}$$

where $\bar{Z}$ is the feeder 2 load impedance. In the normal operation mode, $|\bar{Z}_{K(N)}|$ is greater than $|\bar{Z}_S + \bar{Z}_t|$ because the load is connected to F2. So, the PCC voltage has a constant value, almost equal to the source voltage. During fault, the magnitude ($V_{\mathrm{PCC}(F)}$) and phase angle ($\varphi_{\mathrm{PCC}(F)}$) of PCC voltage is changed and can be expressed by (8) and (9), as follows:

$$V_{\mathrm{PCC}(F)} = \left| \frac{\bar{Z}_{K(F)}}{\left(\bar{Z}_S + \bar{Z}_t\right) + \bar{Z}_{K(F)}} \right| \left|\bar{V}_S\right| \tag{8}$$

$$\varphi_{\mathrm{PCC}(F)} = \arctan\left(\frac{X_{K(F)}}{R_{K(F)}}\right) - \arctan\left(\frac{X_{K(F)} + X_S + X_t}{R_{KF} + R_S + R_t}\right). \tag{9}$$

By calculating the parallel feeders' impedance during the fault, (10) can be obtained

$$\bar{Z}_{K(F)} = \left(\bar{Z}_{L1} + \bar{Z}_{SL}\right) \| \left(\bar{Z}_{L2} + \bar{Z}_F\right) \tag{10}$$

where, Z_F represents the fault impedance. In the fault condition Z_F is approximately equal to zero and according to (10), $|\bar{Z}_{K(F)}|$ will be small. Consequently, voltage sag and phase-angle jump occur in the fault interval. In this situation, the sensitive load experiences the worst condition. To prevent the voltage sag and phase angle jump during the fault, one solution is to place TBSSFCL between PCC and fault location. By connecting TBSSFCL in F2, $V_{\mathrm{PCC(TBSSFCL)}}$ and $\varphi_{\mathrm{PCC(TBSSFCL)}}$ will be obtained as given in (11) and (12). In this case, $Z_{K(\mathrm{TBSSFCL})}$ includes the TBSSFCL impedance as given by (13), and this increased impedance can improve the PCC voltage and phase angle successfully

$$V_{\mathrm{PCC(TBSSFCL)}} = \left| \frac{\bar{Z}_{K(\mathrm{TBSSFCL})}}{\left(\bar{Z}_S + \bar{Z}_t\right) + \bar{Z}_{K(\mathrm{TBSSFCL})}} \right| \left|\bar{V}_S\right| \tag{11}$$

$$\varphi_{\mathrm{PCC(TBSSFCL)}} = \arctan\left(\frac{X_{K(N)}}{R_{K(N)}}\right) - \arctan\left(\frac{X_{K(\mathrm{TBSSFCL})} + X_S + X_t}{R_{K(\mathrm{TBSSFCL})} + R_S + R_t}\right) \tag{12}$$

$$Z_{K(N)} = \left(\bar{Z}_{L1} + \bar{Z}_{SL}\right) \| \left(\bar{Z}_{L2} + \bar{Z}_{\mathrm{TBSSFCL}}\right). \tag{13}$$

C. Power Losses Calculation

For TBSSFCL power loss calculation, the proposed radial distribution network is analyzed in normal and fault operation modes. TBSSFCL has losses in the series transformer, anti-parallel IGBTs and the controlling circuit. Therefore, TBSSFCL power losses during normal operation mode can be calculated as follows:

$$P_{\mathrm{loss}} = P_{Tr} + P_{sw} = P_{\mathrm{core}} + \left(R_{Tr} I_{\mathrm{Line}}^2\right) + V_{\mathrm{IGBT}} I_{\mathrm{Line}} \tag{14}$$

where P_{Tr} is the series transformer power loss, P_{sw} is the two anti-parallel IGBTs losses, R_{Tr} is the transformer equivalent resistance, V_{IGBT} is the forward voltage drop on the IGBT during on state and I_{Line} is the line current, which passes through the IGBTs and series transformer. Nevertheless, the total power loss of the TBSSFCL during normal operation mode is negligible. In order to determine the ac reactor power loss during fault, the ratio of power loss of the ac reactor to active power of the electrical load is defined by the parameter K and can be derived as follows:

$$K = \frac{P_{\mathrm{losses}}}{P_{\mathrm{load}}} = \frac{2 r_d I_{\mathrm{Line}}^2}{r_L I_{\mathrm{line}}^2} = \frac{2 r_d}{r_L} = \frac{r_d I_{\mathrm{Line}}^2}{U_L I_L \cos\varphi} \tag{15}$$

where

$$P_{\mathrm{load}} = r_L \frac{I_{\mathrm{line}}^2}{2}. \tag{16}$$

As an example, in a distribution feeder with the fault current limited to 250 A, power factor = 0.9, $r_d = 0.02\ \Omega$, and $U_L =$ 20 kV, the value of K is equal to 0.27%. Considering (14), the total power loss in the resistance of ac reactor is a very small percentage of the distribution feeders' transmitted power. Note

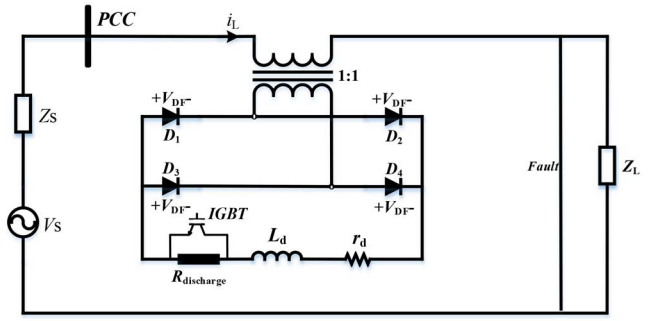

Fig. 3. Single line diagram of the network including SSFCL used in [4], [6], [12], and [16].

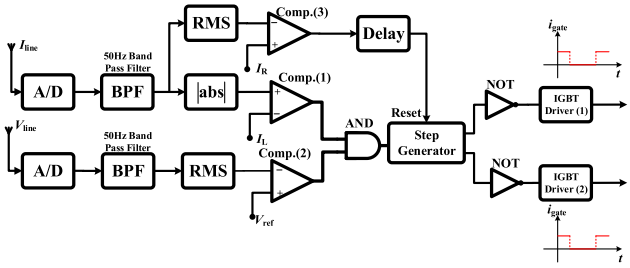

Fig. 4. Control system block diagram.

that the fault condition lasts for a few cycles and has a small time interval.

Comparing the proposed TBSSFCL with the SSFCL suggested in [4], [6], [12], [16], and [27], indicates its superiority in the normal and fault condition losses, as well as the switching overvoltage. For this purpose, the single line diagram of the network, including SSFCL, introduced in [4], [6], [12], and [16], is shown in Fig. 3.

This SSFCL includes a full bridge rectifier, a dc reactor, a damping resistor and an IGBT, all placed at the transformer's secondary side. In normal operating mode, IGBT is on and damping resistor ($R_{\text{discharge}}$) is bypassed. So, the rectifier output causes the dc reactor to show negligible impedance. Fault occurrence causes the current to increase rapidly which is opposed by the dc reactor and provides sufficient time for the controller to take action. Then, the controller opens IGBT and puts the damping resistance in the circuit; therefore fault current is restricted. Although, this SSFCL effectively limits fault current, however, there are some serious problems with its operation. Firstly, IGBTs turn on and off causes very high switching overvoltage. Secondly, flowing high current through the damping resistor produces very high power loss. These points are two important disadvantages of the mentioned SSFCL.

As claimed in [4], [6], [12], and [16], the main advantage of this SSFCL is the control of on and off periods of IGBT, such that the controller can maintain the fault-current amplitude below a specified level. The disadvantage of this SSFCL is its considerable normal and fault conditions power losses which lower its efficiency. In addition, it needs sophisticated control strategy and cooling system.

The proposed TBSSFCL, however, has less power loss during normal and fault conditions, lower initial cost and easier maintenance.

The stored energy in the ac reactor during the fault is an important issue which should be taken into account. It depends on magnitude of the limited fault current and inductance of the reactor. Small reactor stores less energy but cannot sufficiently limit the fault current. Because of alternating nature of the line current, the ac reactor is alternately changed and discharged. After fault, the stored energy should be decreased without any interruption in the system operation. There are some solutions for damping this energy, including gradual discharge in the electrical load, discharging in the transmission line filter, discharging in the neutral point of the transformer and discharging via the anti-parallel IGBTs. Another solution to dissipate the reactor energy is application of dynamic voltage restorer, to return this energy to the PCC.

In this paper, after fault clearance, the control circuit bypasses TBSSFCL with half cycle delay. This delay not only discharges the reactor energy, but also guarantees the system protection against immediate short circuit. Repetitive faults before bypassing the TBSSFCL cannot increase the fault current because TBSSFCL is still connected in series with the line.

D. Control System

Control block diagram of TBSSFCL is shown in Fig. 4.

In order to control TBSSFCL, the line current (i_{Line}) is sampled via a current transformer and is sent to the control circuit. Before comparing i_{Line} with the maximum permissible current level (I_L), it is passed through a 50 Hz band pass filter and its absolute value is sent to comparator (1). Monitoring the instantaneous value of line current increases the controller response speed to the fault occurrence. Also the line voltage (V_{Line}) is measured through a potential transformer and its root mean square (RMS) value is compared with the reference value (V_{ref}) in comparator (2). In this paper, V_{ref} is set to 0.8 p.u., as it is required for motor starting and below this value motor cannot operate. In normal operating mode i_{Line} and i_L, and V_{Line} and V_{ref} are in marginal level and the step generator output pulses turn the IGBTs on. So, the secondary of isolating transformer is short circuited and TBSSFCL shows negligible impedance. At fault inception, as i_{Line} exceeds i_L, the control circuit detects abnormal condition. If the voltage control section also detects sever voltage drop, the step generator turns the anti-parallel IGBTs off and inserts the ac reactor into the current path, which increases the circuit impedance, resulting in fault current limitation. A third control loop can be formed by getting a feedback from the line current RMS value. The line current is applied to a RMS calculating block, the output of which is compared with the reference current level (i_R). At the fault removal, while the anti-parallel switches are still OFF, the RMS value of line current decreases rapidly below the reference value i_R. The detector circuit will then send the reset signal to the step generator block and this block generates the command signal for IGBTs after a half cycle delay. As a result, the system returns to its normal operation mode and TBSSFCL switches turn on again. Combination of the three command signals (voltage, instantaneous current, and

TABLE I
PARAMETERS OF THE RADIAL DISTRIBUTION NETWORK EQUIPPED WITH TBSSFCL

Parameters	Description	Value
V_s	Source Voltage (Line-Line) rms	20kV
r_s	Source Resistance	1Ω
L_s	Source Inductance	0.01H
r_L	Line Resistance	1Ω
L_L	Line Inductance	0.01H
f	Power System Frequency	50Hz
V_{IGBT}	Voltage Drop Across IGBT	2V
r_d	AC Reactor Resistance	0. 02 Ω
L_d	AC Reactor Inductance	0.2H
a	Isolation Transformer Turn Ratio	1:1
R_{load}	Load Resistance	400 Ω
L_{load}	Load Inductance	0.1H

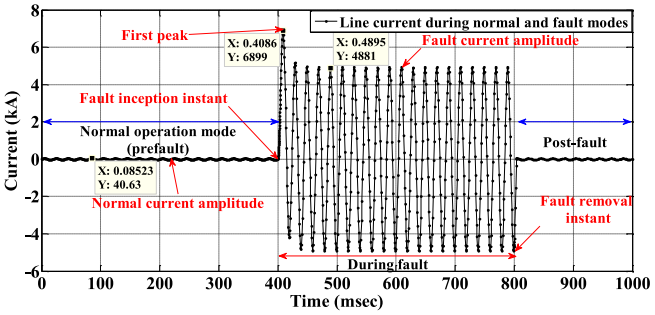

Fig. 5. Line current during normal and fault conditions with no FCL in use.

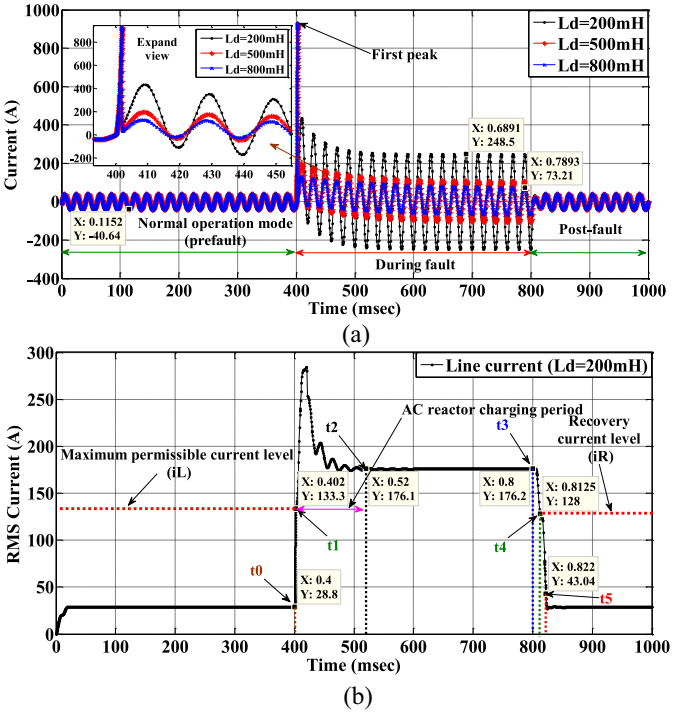

Fig. 6. Line current before, during and after fault with TBSSFCL. (a) Instantaneous. (b) RMS value.

RMS current control loops), as the input signals to the step generator block, generates the appropriate drive signals for IGBTs. This control logic guarantees TBSSFCL proper operation during normal and fault conditions. It can also detect motor starting and transformer energization inrush currents, to prevent TBSSFCL malfunction. Although, TBSSFCL operation during motor starting and transformer energization can reduce overcurrent amplitude and may have some advantages for distribution networks, however, it may increase the start time of motors.

IV. SIMULATION RESULTS

In this section, the system shown in Fig. 1, is used for simulations. Parameters of the system including TBSSFCL are listed in Table I. Simulation is performed for normal and single phase to ground fault conditions. Also, the system source is solidly grounded.

A. Results in the Absence of TBSSFCL

Fig. 5 shows the line current in normal and faulty operation modes, when no FCL is used in the system. The line current has its nominal amplitude of about 40 A during the normal mode. Fault occurrence causes a large increase in the amplitude of the line current, up to about 5 kA, with the first peak of about 6.8 kA.

B. Effect of TBSSFCL

When TBSSFCL is placed in the system, considerable reduction in the fault current is achieved, as shown in Fig. 6. This figure illustrates the instantaneous and RMS values of the line current before, during and after fault, for different values of reactor inductance. As expected, the amount of fault current limitation depends on the value of reactor inductance.

As shown in these figures, before fault occurrence, normal current flows through the line. At t_0 fault starts, causing the line current to increase rapidly, until t_1, at which it reaches I_L. Between t_0 and t_1 the semiconductor switches are still on and TBSSFCL has not operated, allowing the line current to increase. At t_1 the control system turns the IGBTs off and places the ac reactor in the circuit. From instant t_1 to t_2, there is a transient period in which the dc component of current is decayed. At t_3 fault is cleared and the power circuit returns to its normal condition. Therefore, the line current is decreased to the recovery level (i_R) at t_4, when the control circuit detects fault clearance, but it turns on IGBTs after a half cycle delay at t_5. At last, the line current is reduced to the prefault value and the system operates under normal condition. Thus, from t_1 to t_3 is the duration of fault limiting mode and between t_3 and t_5 both electrical load and TBSSFCL are connected to the network. Fig. 7 shows the gate signal, which is applied to both IGBTs with separate drivers.

Fig. 8 shows the ac reactor current during normal and faulty conditions. As it is seen here, the ac reactor is bypassed during normal operation mode, while in the fault condition, it contains the fault current with the first peak of about 400 A, decayed to a steady value of 250 A after a few cycles of transient period.

Fig. 9 shows IGBT switching overvoltage and dc reactor current of the FCL suggested in [4], [6], [12], and [16]. As shown here, there is no fault in the system before $t = 400$ ms and after that the occurred fault increases the

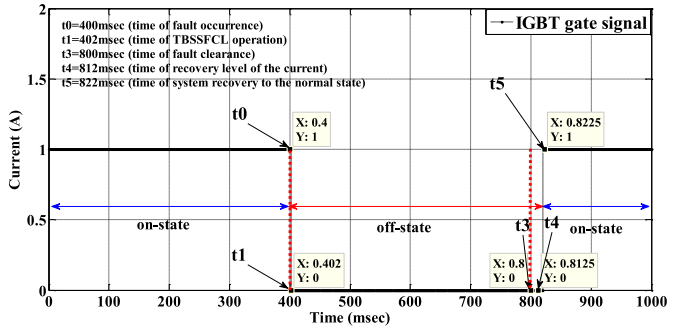

Fig. 7. IGBT gate signal.

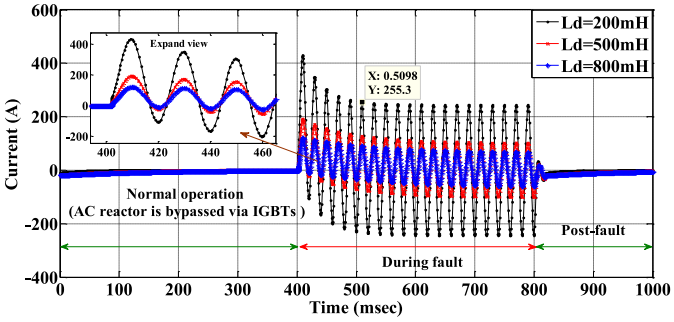

Fig. 8. AC reactor current for different inductance values.

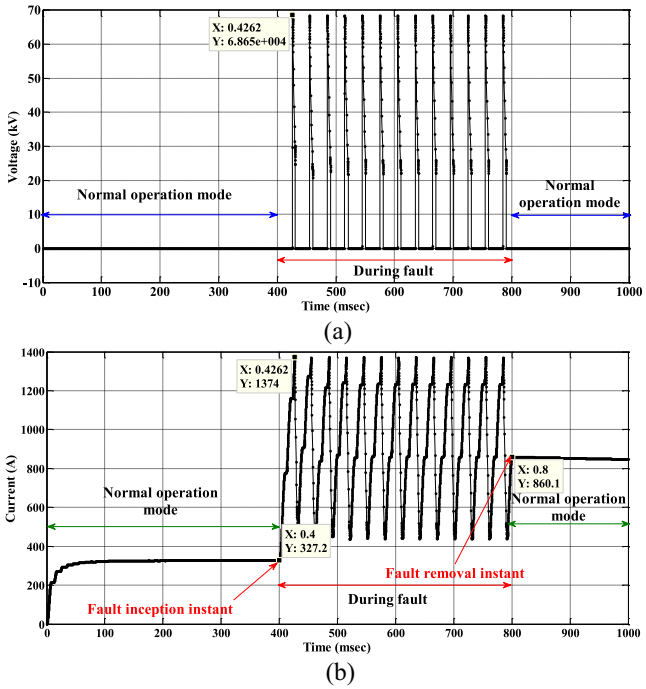

Fig. 9. (a) IGBT switching overvoltage. (b) DC reactor current.

line current. So, IGBT inserts the damping resistor into the line and decreases the fault current below the specified level. Meanwhile, overvoltage with 70 kV amplitude is experienced by IGBT during the fault. Fig. 9(b) shows the reactor current which is the sum of IGBT and damping resistor currents during normal operation and fault. Before fault inception, IGBT is on and damping resistor is bypassed. So, dc current passes

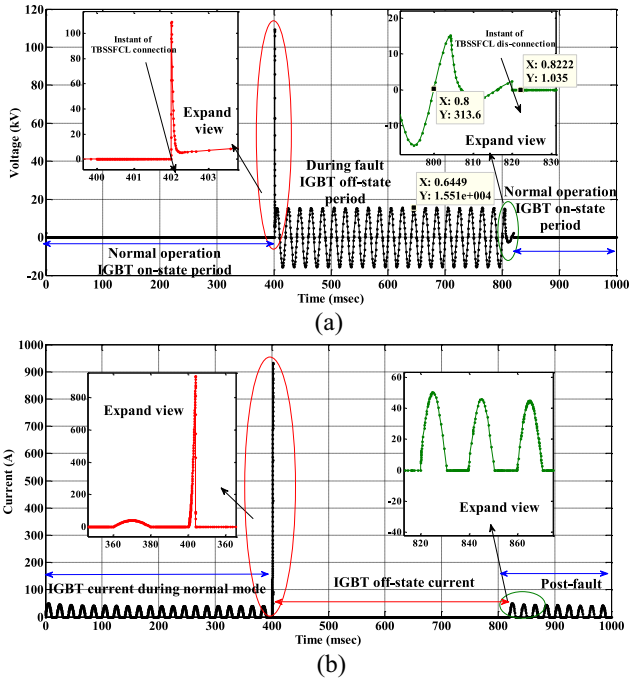

Fig. 10. IGBTs (a) voltage and (b) current during normal and faulty operation modes.

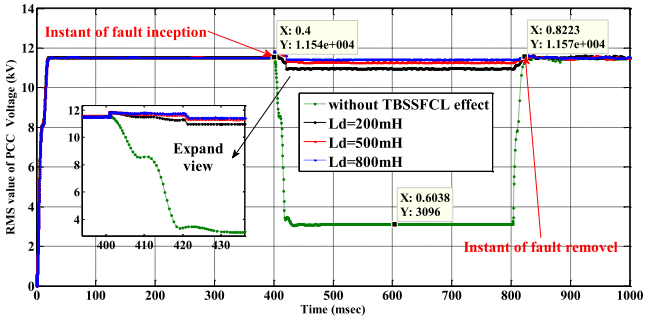

Fig. 11. PCC voltage sag during normal and faulty operation modes with and without TBSSFCL.

via IGBT. After fault inception, the control circuit turns-off IGBT and current flows through the damping resistor. As shown in this figure, the amplitude of damping resistor current reaches 1400 A and causes considerable power loss in the resistor. Furthermore, the high power loss of this FCL needs a suitable cooling system which increases its cost.

Fig. 10 shows TBSSFCL switching overvoltage. It is observed that TBSSFCL reduces switching overvoltage successfully and the voltage amplitude is equal to the nominal peak voltage of the network. According to this figure, there is no power quality distortion and in normal operation mode, the voltage drop on TBSSFCL is negligible.

In addition, IGBTs are in on state in normal operation mode, so the voltage drop of these switches is negligible too. Fig. 11 shows the PCC voltage sage during normal and faulty operation modes. The dotted curve shows the voltage sag when there is no TBSSFCL in the line and the solid curves show TBSSFCL effect on voltage sag at PCC with different value of the ac reactor. TBSSFCL operation has a considerable effect on voltage sag as shown in this figure.

TABLE II
EXPERIMENTAL SETUP PARAMETERS

Transformer Specification	110V,50Hz, 110V/110V, 1kVA	
Transformer short circuit test (SCT)	P(wattmeter)	60W
	V(voltmeter)	11V
	I(ampere meter)	6A
Transformer open circuit test (OCT)	P(wattmeter)	20W
	V(voltmeter)	110V
	I(ampere meter)	0.5A
V_s	Source Voltage (rms)	110V
Distribution feeders data	Feeder F1	0.314j Ω
	Feeder F2	0.157j Ω
Load data	Sensitive load	10+j15.7 Ω
	Load of F2	95+j31.4 Ω
Anti-parallel switches Data	IGBT	600V
		20A
AC reactor Data	AC reactor inductance	0.02H
	AC reactor resistance	0.2Ω
R_{cL}	Transformer core loss equivalent resistance	484.048Ω
X_{mL}	Magnetization Branch Reactance	246.99Ω
r_{eL}	winding resistance	0.016 Ω
X_{eL}	Leakage reactance	0.65 Ω

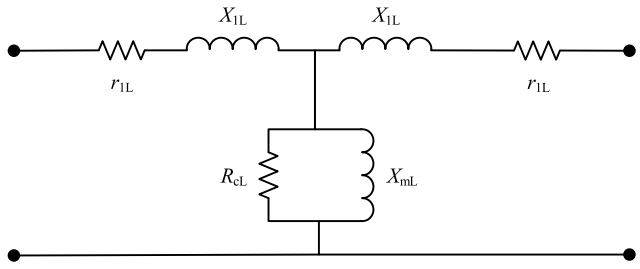

Fig. 12. Transformer equivalent model.

V. EXPERIMENTAL RESULTS

An experimental setup, based on Fig. 1, is implemented in laboratory. This prototype consists of a transformer with 1:1 turn ratio, 110 V/110 V, used as the coupling series transformer. Table II lists the transformer open circuit and short circuit tests results. Also, other proposed system parameters are listed in this table.

The transformer equivalent circuit is shown in Fig. 12.

The implemented prototype including the electrical load is shown in Fig. 13.

Using a start/stop switch, a single line to ground fault is simulated. The control circuit includes a current sensor (LTS25-NP) which is connected in series with the line for monitoring the line current during normal and fault conditions. Output of this sensor is applied to an microcontroller for analyzing the line current and producing command signals for IGBTs. There are two IGBT gate drivers.

Fig. 14 shows the line current and load voltage before and after fault occurrence. Fault occurs at Fig. 14(a) and is removed at Fig. 14(b). Before fault occurrence, the line current amplitude is 1 A and the load voltage is 110 V. The load voltage and line current are sinusoidal and system operates under normal condition. In this case, the two anti-parallel IGBTs are in on state and the voltage drop on TBSSFCL is

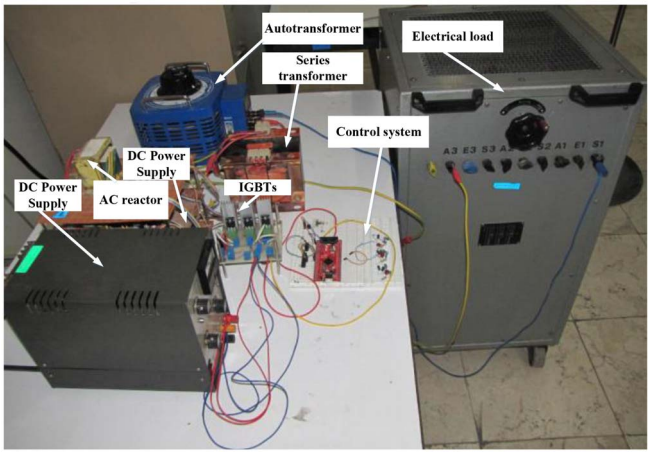

Fig. 13. Laboratory test system including TBSSFCL.

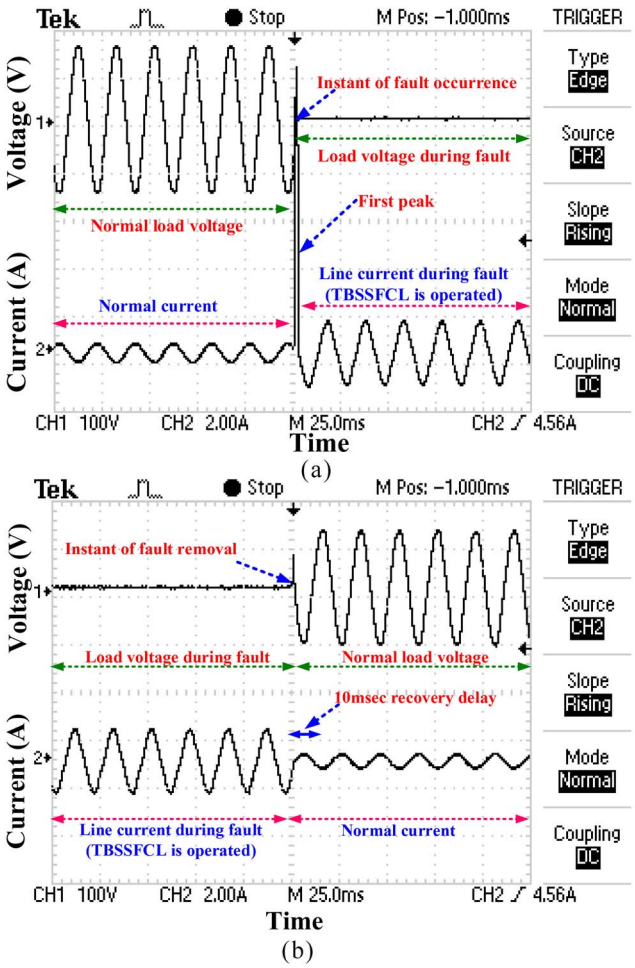

Fig. 14. TBSSFCL effect on line current (lower curve: current/division = 2 A and time/division = 25 ms) and load voltage (upper curve: voltage/division = 100 V) before and after fault occurrence [fault incepts at (a) and is removed at (b)].

negligible. At the instant of fault inception, the line current is sharply increased, but TBSSFCL immediately reacts and the drivers change the IGBTs gates signals to zero, causing the IGBTs to turn off. Thus, the ac reactor is connected to the secondary side of the series transformer and the amplitude of the fault current is decreased to 2 A. After fault removal,

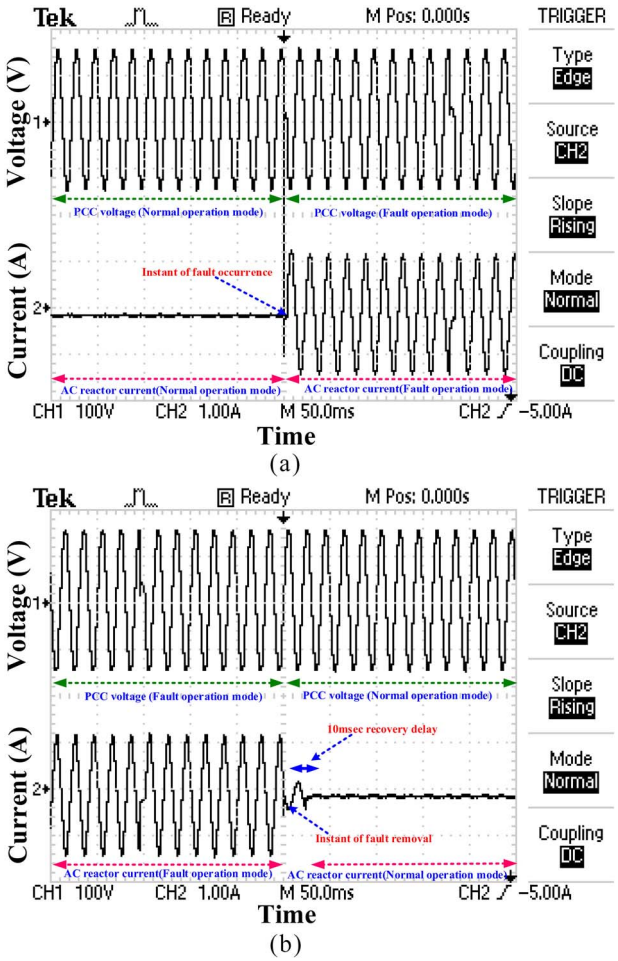

Fig. 15. AC reactor current (lower curve, current/division = 1A with probe X1 (Oscilloscope probe coefficient is one) for CH2 (channel two of the digital oscilloscope) and time/division = 50 ms) and PCC voltage (upper curve, voltage/division = 100 V with probe X1 (Oscilloscope probe coefficient is one) for CH1 (Oscilloscope probe coefficient is one) and time/division = 50 ms) during normal and fault operation modes.

the fault current is decreased to the acceptable level and again anti-parallel switches turn on and TBSSFCL returns to its normal mode. Fig. 14 is in a good agreement with Fig. 6.

Fig. 15 shows the ac reactor current and PCC voltage before, during and after fault. As shown in this figure, TBSSFCL can successfully control the fault current and also can fix the PCC voltage to an acceptable level.

In addition, the experimental results shown in Fig. 15 are in agreement with the simulation results depicted in Figs. 8 and 11. During normal operation mode, the measured PCC voltage is 110 V (RMS) and TBSSFCL has negligible effect on the voltage waveform. At fault condition also, TBSSFCL has restored PCC voltage to an acceptable level.

The IGBTs switching frequency and duty cycle play important role in TBSSFCL operation. Therefore, the voltage drop and current of these switches are of interest. Fig. 16 shows the IGBTs current and voltage during normal and faulty operation modes. As shown in Fig. 16, fault is removed at Fig. 16(b) but the control circuit turns on IGBTs after half cycle (10 ms). This ensures safe operation of the system because in this half cycle both TBSSFCL and electrical load are connected to the line and the stored energy in the ac reactor is decreased.

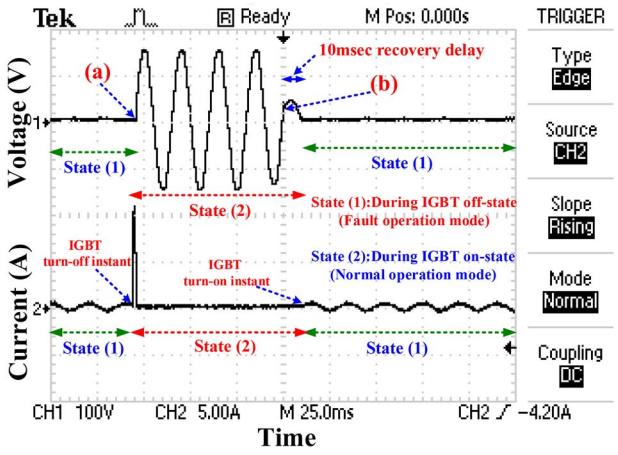

Fig. 16. Voltage (upper curve: voltage/division = 100 V with probe X1 for CH1 and time/division = 25 ms) and current across IGBTs (lower curve: current/division = 5 A with probe X1 for CH2 and time/division = 25 ms) during normal and faulty operation mode [fault incepts at (a) and is removed at (b)].

IGBT is a suitable power electronic switch for use in low power applications and is available with voltage rating of up to 6.5 kV, both in press-pack and modules [29]. Also, series-parallel connections of semiconductor switches have recently been proposed to satisfy the requirements of a wide range of voltage and current levels. IGCTs are also available in the voltage levels from 2.5 to 10 kV and current level up to 9 kA [30]. Since IGCTs on-state power losses are low, they can be used in high power application [30]. Nevertheless, the design procedure of the switches and their selection for a special network is not in the scope of this paper.

VI. Conclusion

In this paper, a novel FCL configuration, called TBSSFCL, has been proposed. The main advantages of the proposed TBSSFCL are its lower switching overvoltage and power loss, compared with other recently suggested SSFCLs, which have high power loss in damping resistor and require cooling system. Omitting the diode bridge rectifier, cooling system and damping resistor results in lower initial cost in the suggested TBSSFCL. Simpler structure also guaranties safe and reliable operation. Simulation and experimental results have shown the TBSSFCL capabilities in fault current limitation in radial distribution network application.

References

[1] J. McAullife, D. Amin, I. Peacock, and D. Durocher, "Optimizing capital costs in power-distribution upgrades," *IEEE Ind. Appl. Mag.*, vol. 7, no. 5, pp. 41–51, Aug./Sep. 2001.

[2] Z. Yang *et al.*, "Dynamic simulation of the overvoltage for fault current limiter," in *Proc. Asia-Pac. Power Energy Eng. Conf. (APPEEC)*, Wuhan, China, 2011, pp. 1–4.

[3] C. S. Chang and P. C. Loh, "Integration of fault current limiters on power systems for voltage quality improvement," *Elect. Power Syst. Res.*, vol. 57, no. 2, pp. 83–92, 2001.

[4] M. Abapour and M. T. Hagh, "A non-superconducting fault current limiter with controlling the magnitudes of fault currents," *IEEE Trans. Power Electron.*, vol. 24, no. 3, pp. 613–619, Mar. 2009.

[5] M. T. Hagh and M. Abapour, "DC reactor type transformer inrush current limiter," *IET Elect. Power Appl.*, vol. 1, no. 5, pp. 808–814, Sep. 2007.
[6] M. Firouzi, G. B. Gharehpetian, and M. Pishvaei, "A dual-functional bridge type FCL to restore PCC voltage," *Elect. Power Energy Syst.*, vol. 46, pp. 49–55, Mar. 2013.
[7] A. Abramovitz and K. M. Smedley, "Survey of solid-state fault current limiters," *IEEE Trans. Power Electron.*, vol. 27, no. 6, pp. 2770–2782, Jun. 2012.
[8] H. Radmanesh, S. H. Fathi, and G. B. Gharehpetian, "Novel high performance DC reactor type fault current limiter," *Elect. Power Syst. Res.*, vol. 122, pp. 198–207, May 2015.
[9] M. Steurer, K. Frohlich, W. Holaus, and K. Kaltenegger, "A novel hybrid current-limiting circuit breaker for medium voltage: Principle and test results," *IEEE Trans. Power Del.*, vol. 18, no. 2, pp. 460–467, Apr. 2003.
[10] W. Fei, Y. Zhang, and Z. Lu, "Novel bridge-type FCL based on self-turnoff devices for three-phase power systems," *IEEE Trans. Power Del.*, vol. 23, no. 4, pp. 2068–2078, Oct. 2008.
[11] W. Fei and Y. Zhang, "A novel IGCT-based half-controlled bridge type fault current limiter," in *Proc. CES/IEEE 5th Int. Power Electron. Motion Control Conf. (IPEMC)*, vol. 2. Shanghai, China, 2006, pp. 1–5.
[12] M. Firouzi and G. B. Gharehpetian, "Improving fault ride-through capability of fixed-speed wind turbine by using bridge-type fault current limiter," *IEEE Trans. Energy Convers.*, vol. 28, no. 2, pp. 361–369, Jun. 2013.
[13] M. M. Lanes, H. A. C. Braga, and P. G. Barbosa, "Fault current limiter based on resonant circuit controlled by power semiconductor devices," *IEEE Latin America Trans.*, vol. 5, no. 5, pp. 311–320, Sep. 2007.
[14] M. M. R. Ahmed, G. Putrus, L. Ran, and R. Penlington, "Development of a prototype solid-state fault-current limiting and interrupting device for low-voltage distribution networks," *IEEE Trans. Power Del.*, vol. 21, no. 4, pp. 1997–2005, Oct. 2006.
[15] W. Fei, Y. Zhang, and Z. Meng, "A novel solid-state bridge type FCL for three-phase three-wire power systems," in *Proc. 22nd Annu. IEEE Appl. Power Electron. Conf.*, vol. 2. Anaheim, CA, USA, 2007, pp. 1084–1088.
[16] S. B. Naderi, M. Jafari, and M. T. Hagh, "Controllable resistive type fault current limiter (CR-FCL) with frequency and pulse duty-cycle," *Int. J. Elect. Power Energy Syst.*, vol. 61, pp. 11–19, Oct. 2014.
[17] J.-F. Moon and J.-S. Kim, "Voltage sag analysis in loop power distribution system with SFCL," *IEEE Trans. Appl. Supercond.*, vol. 23, no. 3, Jun. 2013, Art. ID 5601504.
[18] S. Najafi, V. K. Sood, and A. Hosny, "Effect of static fault current limiter on distribution power quality," in *Proc. IEEE Elect. Power Energy Conf. (EPEC)*, London, ON, Canada, 2012, pp. 26–31.
[19] A. Agheli, H. A. Abyaneh, R. M. Chabanloo, and H. H. Dezaki, "Reducing the impact of DG in distribution networks protection using fault current limiters," in *Proc. 4th Int. Power Eng. Optim. Conf. (PEOCO)*, Shah Alam, Malaysia, 2010, pp. 298–303.
[20] S.-Y. Kim, W.-W. Kim, and J.-O. Kim, "Determining the location of superconducting fault current limiter considering distribution reliability," *IET Gener. Transmiss. Distrib.,* vol. 6, no. 3, pp. 240–246, Mar. 2012.
[21] S. Hemmati and J. Sadeh, "Applying superconductive fault current limiter to minimize the impacts of distributed generation on the distribution protection systems," in *Proc. 11th Int. Conf. Environ. Elect. Eng. (EEEIC)*, Venice, Italy, 2012, pp. 808–813.
[22] M. M. R. Ahmed, "Comparison of the performance of two solid state fault current limiters in the distribution network," in *Proc. 4th IET Conf. Power Electron. Mach. Drives (PEMD),* York, U.K., 2008, pp. 772–776.
[23] V. K. Sood and R. Amin, "EMTP RV-based study of solid-state fault current limiter for distribution systems," in *Proc. IEEE Power India Conf.*, New Delhi, India, 2006, pp. 6–12.
[24] R. J. Yinger, S. S. Venkata, and V. A. Centeno, "Southern California Edison's advanced distribution protection demonstrations," *IEEE Trans. Smart Grid*, vol. 3, no. 2, pp. 1012–1019, Jun. 2012.
[25] J. R. Prigmore, J. A. Mendoza, and G. G. Karady, "A neodymium hybrid fault current limiter," *Int. Trans. Elect. Energy Syst.*, to be published.
[26] J.-Y. Yoon, S.-R. Lee, and I.-T. Hwang, "A quantitative analysis on future world marketability of HTS power industry," *IEEE Trans. Smart Grid*, vol. 4, no. 1, pp. 433–436, Mar. 2013.
[27] A. R. Fereidouni, B. Vahidi, and T. H. Mehr, "The impact of solid state fault current limiter on power network with wind-turbine power generation," *IEEE Trans. Smart Grid*, vol. 4, no. 2, pp. 1188–1196, Jun. 2013.
[28] C. Becker *et al.*, "Proposed chapter 9 for predicting voltage sags (dips) in revision to IEEE Std 493, the gold book," *IEEE Trans. Ind. Appl.*, vol. 30, no. 3, pp. 805–821, May/Jun. 1994.
[29] M. Rahimo, A. Kopta, and S. Linder, "Novel enhanced-planar IGBT technology rated up to 6.5kV for lower losses and higher SOA capability," in *Proc. Int. Symp. Power Semiconduct. Devices ICs (ISPSD),* Napoli, Italy, 2006, pp. 1–4.
[30] ABB Semiconductors. (Apr. 2014). [Online]. Available: http://www.abb.com/ semiconductors

Hamid Radmanesh (S'09–A'12) was born in 1981. He received the B.Sc. degree in telecommunication engineering from the Malek-Ashtar University of Technology, Tehran, Iran, in 2006, and the M.Sc. and Ph.D. degrees in electrical engineering from Shahed University, Tehran, and the Amirkabir University of Technology (Tehran Polytechnic) University, Tehran, in 2006 and 2015, respectively.

His current research interests include design and modeling of power electronic converters and FCLs, drives, transient in power system, and chaos in power system apparatus. He has authored over 50 journal and conference papers.

Hamid Fathi (S'90–M'00) received the B.Sc. degree from the Amirkabir University of Technology (AUT), Tehran, Iran, the M.Sc. degree from the Iran University of Science and Technology, Tehran, and the Ph.D. degree from the University of Newcastle upon Tyne, Newcastle Upon Tyne, U.K., in 1984, 1987, and 1991, respectively, all in electrical engineering.

He is currently an Associate Professor with the Department of Electrical Engineering, AUT. His current research interests include power quality, flexible ac transmission systems, power electronics, and electric drives.

Gevork B. Gharehpetian (M'00–SM'08) received the B.Sc. degree from Tabriz University, Tabriz, Iran; the M.Sc. degree from the Amirkabir University of Technology (AUT), Tehran, Iran; and the Ph.D. degree from Tehran University, Tehran, in 1987, 1989, and 1996, respectively, all in electrical engineering.

From 1997 to 2003, he was an Assistant Professor, an Associate Professor from 2004 to 2007, and has been a Professor since 2007 at AUT. He has authored over 700 journal and conference papers. His current research interests include smart grid, DGs, monitoring of power transformers, FACTS devices, HVDC systems, and power system transients.